Development and characteristics analysis of recessed-gate MOS HEMT*

Wang Chong(王冲)†, Ma Xiaohua(马晓华), Feng Qian(冯倩), Hao Yue(郝跃),
Zhang Jincheng(张进城), and Mao Wei(毛维)

(Key Laboratory of Wide Band-Gap Semiconductor Materials and Devices, School of Microelectronics, Xidian University, Xi'an 710071, China)

Abstract: An AlGaN/GaN recessed-gate MOSHEMT was fabricated on a sapphire substrate. The device, which has a gate length of 1 μm and a source-drain distance of 4 μm, exhibits a maximum drain current density of 684 mA/mm at V_{gs} = 4 V with an extrinsic transconductance of 219 mS/mm. This is 24.3% higher than the transconductance of conventional AlGaN/GaN HEMTs. The cut-off frequency and the maximum frequency of oscillation are 9.2 GHz and 14.1 GHz, respectively. Furthermore, the gate leakage current is two orders of magnitude lower than for the conventional Schottky contact device.

Key words: high electron mobility transistors; AlGaN/GaN; recessed-gate; dielectric gate
DOI: 10.1088/1674-4926/30/5/054002 **PACC:** 7340N; 7360L; 7320 **EEACC:** 2520D; 2530C

1. Introduction

High-performance AlGaN/GaN HEMTs on sapphire or SiC substrates have been successfully applied to microwave power devices[1, 2]. To date, research has focused on the MOSHEMT or recessed-gate devices. In the dielectric gate devices, the leakage current has been reduced significantly and the larger maximum drain current was obtained for a higher positive gate bias[3]. However, the transconductance has been decreased and the threshold voltage shifted to negative direction values[4]. In recessed-gate devices, as a part of the AlGaN layer under the gate has been etched, the devices' transconductance is improved[5], but the leakage current of the gate will be increased due to the etching damage[6]. Recently, Nakamura[7] reported on the fabrication of a recessed-gate MISHEMT with a field plate and an output power that reached up to 140 W. In this paper, we describe the recessed-gate AlGaN/GaN MOSHEMT and compare its characteristics with the conventional HEMTs, MOSHEMTs, and recessed-gate devices.

2. Device structure and fabrication

The AlGaN/GaN HEMT used in this paper was grown on a (0001) sapphire substrate in an MOCVD system. The HEMT structure consists of a low-temperature GaN nucleation layer, a 3-μm thick unintentionally doped GaN buffer layer and an AlGaN barrier layer. The barrier layer consists of a 5-nm undoped spacer, a 12-nm carrier supplier layer doped at 2×10^{18} cm^{-3}, and a 5-nm undoped cap layer. Room temperature Hall measurements of the structure yield an electron sheet density of 1.03×10^{13} cm^{-2} and an electron mobility of 1238 cm^2/(V·s). The same materials were used for conventional HEMTs, MOSHEMTs and recessed-gate devices.

The device mesa was formed using Cl_2/N_2 plasma dry etching in an ICP system followed by the source/drain Ohmic contact formation using Ti/Al/Ni/Au (30 nm / 180 nm / 40 nm / 60 nm), annealed at 850 °C for 30 s. The same isolation and ohmic contact processes were used for conventional HEMTs, MOSHEMTs, and recessed-gate MOSHEMTs. After gate windows with 1-μm length were opened by contact photolithography, the recessed-gate MOSHEMT sample was treated with a Cl_2 plasma in an ICP system at an RF plasma bias voltage of 50 V. The recess area was etched at 0.1 nm/s to a depth of 6 nm. The SiO_2 (4 nm) and Ni/Au (30 nm / 200 nm) e-beam evaporation and lift-off were carried out simultaneously to form the gate electrode by using recessed-gate etching mask. The inserted SiO_2 before gate metal evaporation makes the gate contact act as a dielectric gate. The gate length, gate width, and source drain distance are 1, 100, and 4 μm, respectively. Using on-wafer TLM patterns, the contact resistance and the specific contact resistance were measured to be 0.63 Ω·mm and 1.2×10^{-5} Ω·cm^2. The TLM structures were made on the same wafer of the HEMT and located regularly around the device. Direct current characteristics and high frequency characteristics were measured by a HP4156B semiconductor parameter analyzer and an HP8720D network analyzer. Figure 1 shows the structure of our recessed-gate MOSHEMT.

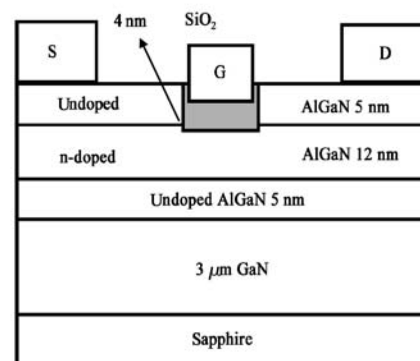

Fig. 1. Cross section of the recessed-gate MOSHEMT.

* Project supported by the National Natural Science Foundation of China (No. 60736033) and the Xi'an Applied Materials Innovation Fund (No. XA-AM-200616).

† Corresponding author. Email: wangchong197810@hotmail.com

Received 24 December 2008, revised manuscript received 14 February 2009 © 2009 Chinese Institute of Electronics

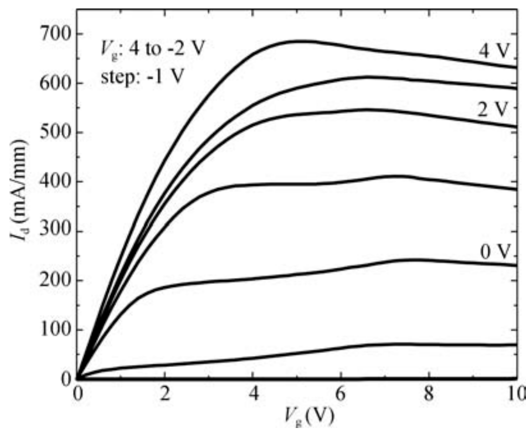

Fig. 2. Output characteristics for the recessed-gate MOSHEMT.

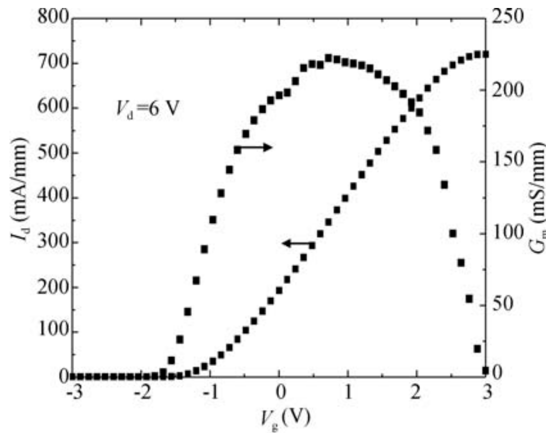

Fig. 3. Transfer characteristics for the recessed-gate MOSHEMT.

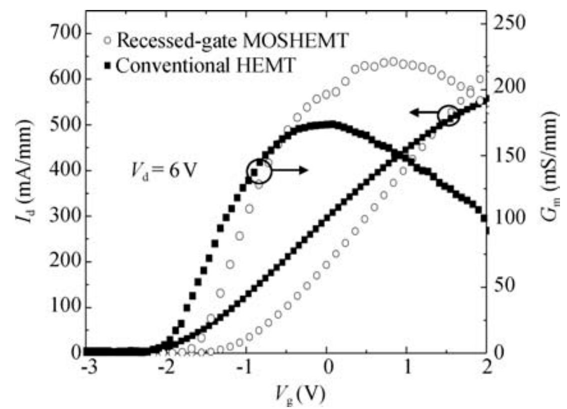

Fig. 4. Transconductance characteristics for a recessed-gate MOSHEMT and a HEMT.

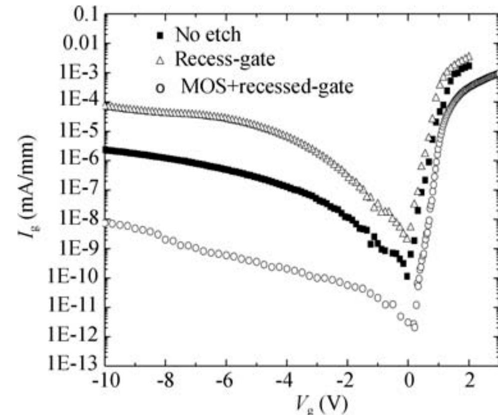

Fig. 5. Gate leakage current for a HEMT, a recessed-gate HEMT, and a recessed-gate MOSHEMT.

3. Results and discussion

Figures 2 and 3 show the output and transfer characteristics of the recessed-gate MOSHEMT, respectively. There are some current uniformity problems in Fig. 2 because there is no passivation layer to eliminate the current collapse during the DC voltage sweep. Because the gate bias voltage of the recessed-gate MOSHEMT can be applied to 4 V and that of the conventional AlGaN/GaN HEMT can be only applied to 2 V, the maximum drain current density of the recessed-gate MOSHEMT reaches 684 mA/mm, which is 22.5% higher than that of the conventional AlGaN/GaN HEMT. On the other hand, because the depth of the etched AlGaN layer was only 6 nm and the reduced density of the 2DEG by using a recessed-gate can be resumed when a sufficiently high positive bias voltage is applied to the gate, the maximum drain current remained at a high value. Using a recessed-gate structure, the distance between the gate and the channel is reduced and the controlling ability of gate increases. So, the peak transconductance of the recessed-gate MOSHEMT is increased from 176 to 219 mS/mm, which is 24.3% higher than that of the conventional AlGaN/GaN HEMT. The SiO_2 dielectric layer inserted between the gate and the AlGaN layer will increase the distance of the gate to the channel; but the SiO_2 layer that we used is only 4 nm. Thus, the impact of the gate dielectric layer on the threshold voltage and the transconductance is very weak, and our experimental results of MOSHEMTs have proven this fact[8].

The threshold voltage of the HEMT can be expressed by[9]

$$V_T = \Phi_B - \frac{\Delta E_C}{q} - \frac{qN_D(d-d_i)^2}{2\varepsilon_0\varepsilon_1} - \frac{\sigma_{pol}}{\varepsilon_0\varepsilon_1}d, \qquad (1)$$

where σ_{pol} is the polarization charge, q is the electron charge, ε_0 is the vacuum permittivity, ε_0 is the relative dielectric constant, $q\Phi_B$ is the Schottky barrier height, ΔE_C is the conduction band offset, N_D is the donor density of AlGaN, d is the total thickness of AlGaN, and d_i is the thickness of the space layer. According to Eq. (1), in a recessed-gate MOSHEMT structure, the dielectric gate structure increases the distance of the gate to the channel. In contrast, the recessed-gate structure reduces the distance. Figure 4 shows the transfer characteristic comparison of a conventional HEMT and a recessed-gate MOSHEMT. The threshold voltage of a recessed-gate MOSHEMT increases by 0.52 V. Due to the weak impact on the threshold voltage of the thin gate dielectric, the positive shift of the threshold is mainly dominated by the recessed-gate mechanism.

Figure 5 shows the $I_g - V_{gs}$ curves of differently structured devices. The gate leakage characteristic of the recessed-gate MOSHEMT is similar to that of a MOSHEMT, which is not shown here. Since a certain etching-induced damage accompanies the plasma treatment of the gate region of the AlGaN layer, the Schottky characteristic of the recessed-gate was aggravated and the leakage current increased by one order of magnitude compared to that of a conventional HEMT due to

Table 1. DC characteristics of different device structures.

	I_{dmax} (mA/mm)	G_{mmax} (mS/mm)	V_{th} (V)	I_g at –10 V (mA/mm)
HEMT	558 at 2 V	176	2.07	1.2×10^{-6}
MOSHEMT	718 at 4 V	172	2.1	8.3×10^{-9}
Recessed-gate HEMT	473 at 2 V	220	1.46	9.3×10^{-5}
Recessed-gate MOSHEMT	684 at 4 V	219	1.55	8.6×10^{-9}

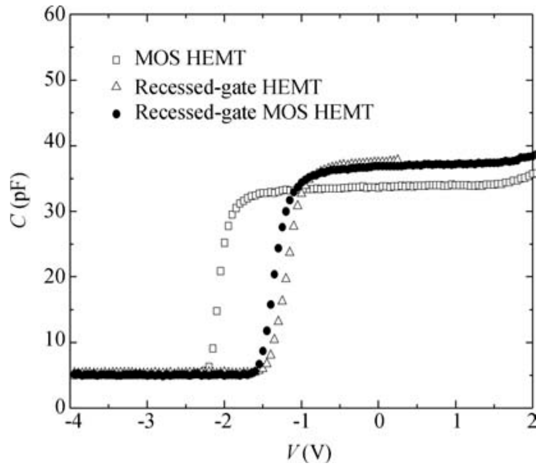

Fig. 6. *C–V* characterization for HEMTs having different structures.

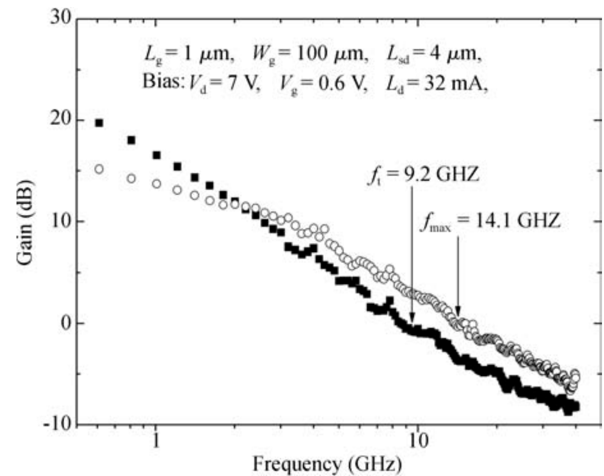

Fig. 7. Gain versus frequency for a MOSHEMT with recessed-gate.

the increase of nitrogen vacancies and surface defects[10]. However, the insertion of SiO_2 between the gate electrode and the etched AlGaN layer decreased the leakage current from 9.3×10^{-5} to 8.6×10^{-9} mA/mm at $V_{gd} = -10$ V. At the same time, the leakage current of the recessed-gate MOSHEMT at positive bias $V_{gs} = 3$ V was below 1 mA/mm, when the leakage current reached 1 mA/mm for the conventional HEMT device at $V_{gs} = 1.5$ V. Table 1 shows the DC characteristics of different device structures.

Figure 6 shows the *C–V* measurement results. The capacitance of a recessed-gate device and a recessed-gate MOSHEMT is almost identical, indicating the insertion of SiO_2 does not influence the gate controlling ability. The capacitance of a MOSHEMT is lower than that of a recessed-gate device and a recessed-gate MOSHEMT, which indicates that using an recessed-gate can increase the gate capacitance. Furthermore, the threshold voltage increases after using the recessed-gate structure but it remains nearly unchanged when the SiO_2 layer was inserted.

On-wafer small-signal RF characteristics of the MOSHEMT with a recessed gate device were measured from 0.1 to 40 GHz, and Figure 7 shows that the cut off frequency and the maximum frequency of oscillation were 9.2 and 14.1 GHz, respectively. The interface states introduced by the recessed gate process have an impact on the frequency characteristic. Further reduction of the etching damage should further improve the frequency characteristics.

4. Conclusion

AlGaN/GaN MOSHEMTs with recessed gates are fabricated on sapphire substrates, The devices with a gate length of 1 μm exhibit an extrinsic transconductance of about 219 mS/mm, which is 24.3% higher than that of the conventional AlGaN/GaN HEMT. The cut off frequency and the maximum frequency of oscillation are 9.2 and 14.1 GHz. The recessed-gate MOSHEMT device structure combines the advantages of the MOS gate structure and the recessed gate, leading to a leakage current of only 8.6×10^{-9} mA/mm at $V_{gd} = -10$ V. For AlGaN/GaN MOSHEMTs, the transconductance is increased by using a recessed-gate and the gate leakage is reduced by using the MOS gate structure. The analysis of the *C–V* characteristic shows that the gate controlling ability increases due to the recessed-gate structure. In addition, the insertion of a dielectric has little impact on the threshold voltage.

References

[1] Kumar V, Kim D H, Basu A, et al. 0.25 μm self-aligned AlGaN/GaN high electron mobility transistors. IEEE Electron Device Lett, 2008, 29(1): 18

[2] Koudymov A, Wang C X, Adivarahan V, et al. Power stability of AlGaN/GaN HFETs at 20 W/mm in the pinched-off operation mode. IEEE Electron Device Lett, 2007, 28(1): 5

[3] Yue Yuanzheng, Hao Yue, Feng Qian, et al. GaN MOS-HEMT using ultra-thin Al_2O_3 dielectric grown by atomic layer deposition. Chin Phys Lett, 2007, 24(8): 2419

[4] Yue Y, Hao Y, Zhang J, et al. AlGaN/GaN MOS-HEMT with HfO_2 dielectric and Al_2O_3 interfacial passivation layer grown by atomic layer deposition. IEEE Electron Device Lett, 2008, 29(8): 838

[5] Okamoto Y, Ando Y, Nakayama T, et al. High-power recessed-gate AlGaN/GaN HFET with a field-modulating plate. IEEE Trans Electron Devices, 2004, 51(12): 2217

[6] Shul R J, Zhang L, Baca A G, et al. Inductively coupled high-density plasma-induced etch damage of GaN MESFETs. Solid-State Electron, 2001, 45 (1): 13

[7] Nakayama T, Ando Y, Okamoto Y, et al. CW 140 W recessed-gate AlGaN/GaN MISFET with field-modulating plate. Elec-

tron Lett, 2006, 42(8): 489

[8] Wang Chong, Yue Yuanzheng, Ma Xiaohua, et al. Development and characteristics analysis of MOS AlGaN/GaN HEMT. Journal of Semiconductors, 2008, 29(8): 1557 (in Chinese)

[9] Drozdovski N V, Caverly R H. GaN-based high electron-mobility transistors for microwave and RF control applications. IEEE Trans Microw Theory Tech, 2002, 50(1): 4

[10] Zhang H, Miller E J, Yu E T. Analysis of leakage current mechanisms in Schottky contacts to GaN and $Al_{0.25}Ga_{0.75}N/GaN$ grown by molecular-beam epitaxy. J Appl Phys, 2006, 99(2): 023703-1